A New Method for Studying the Extraction Kinetics with Monitoring of the Organic Phase Properties by Attenuated Total Reflection IR Spectroscopy

T. S. Aleksandrov[a,b,*], M. D. Karavan[a,b], E. S. Babitova[a,b],
A. A. Brechalov[a,b], and I. V. Smirnov[a,b]

[a] *St. Petersburg State University, St. Petersburg, 198504 Russia*
[b] *Khlopin Radium Institute, St. Petersburg, 194021 Russia*
*e-mail: st077084@student.spbu.ru

Abstract—The kinetics of europium and yttrium extraction with mono- and polyfunctional ligands in organic diluents was studied by attenuated total reflection IR spectroscopy and a method using a diffusion cell. The extraction rate is influenced by the kind of the ligand, solvate formation mechanism, and specific features of diffusion. The extraction rate constants in the systems studied were calculated. In the extraction of europium with organophosphorus ligands, the extraction rate constants range from 3.3×10^{-4} to 1.1×10^{-3} cm s^{-1}. A stepwise complexation mechanism with polyfunctional ligands containing P=O and C=O groups was revealed. In the case of yttrium extraction, the extraction rate constant with a mixed extractant, 2,3-dihydroxynaphthalene + methyltrioctylammonium carbonate, is 1.5×10^{-3} cm s^{-1}, which is higher by an order of magnitude than the rate constant obtained with 8-hydroxyquinoline ($k = 4.3 \times 10^{-4}$ cm s^{-1}), owing to a synergistic effect.

Keywords: extraction kinetics, europium, cesium, yttrium, ATR IR spectroscopy, Lewis cell

DOI: 10.1134/S1066362225050054

INTRODUCTION

Solvent extraction is the most important technique in spent nuclear fuel and radioactive waste reprocessing. It ensures selective recovery of actinides and fission products with organic extractants capable of forming stable complexes with metal ions. The advantages of the extraction are high purity of the products obtained, possibility of performing the process in the continuous mode, efficient recovery of even trace amounts of components, and relatively simple implementation using commercial contactors [1–4].

PUREX process is the most important radiochemical process based on solvent extraction. The process involves the extraction of uranium and plutonium from nitric acid solutions with a solution of tributyl phosphate (TBP) in kerosene. Additional extraction steps allow removal of cesium and strontium and separation of lanthanides and minor actinides, which considerably reduces the radiotoxicity of the final waste forms [5, 6]. When developing industrial extraction systems, it is necessary to take into account not only the thermodynamic characteristics of the process but also its kinetics.

The extraction kinetics describes the rate of the substance transfer between aqueous and organic phases. It is determined by both physical (diffusion) and chemical (complexation, hydration, solvation) processes. One of key factors affecting the kinetics is the presence of diffusion boundary layers at the interface. According to the two-film model suggested by Nernst and Brunner, the substance transfer rate is limited either by diffusion through these films or by the rate of the chemical reaction at the interface [7].

The extraction kinetics is influenced by temperature, pH, reagent concentrations, ionic strength, presence of salting-out agents, and hydrodynamic conditions. The temperature elevation, as a rule, accelerates the process owing to an increase in the diffusion coefficients and rate constants in accordance with the Arrhenius equation. Changes in pH can lead to changes in the metal ion

speciation and to an increase or decrease in the degree of the extractant dissociation, thus altering the complex formation rate and, as a consequence, the extraction rate. An increase in the extractant concentration leads to an increase in the probability of the reaction at the interface, but the effect is leveled off at the interface saturation. The third phase formation and the formation of a stable emulsion at vigorous stirring can also decrease the extraction efficiency, affecting the attainment of the phase equilibrium [7–10].

The most widely used methods for studying the extraction kinetics are described below.

The simplest method is the test tube method in which the organic and aqueous phases are stirred manually or on a shaker and the component distribution is analyzed at definite time intervals. The method allows approximate estimation of the equilibration time and is used in early steps of assessment of extraction systems. It, however, does not allow quantitative description of phase transfer mechanisms [11–13].

One of the most widely used methods is that based on a Lewis diffusion cell. This cell is a glass or plastic vessel with stirring of both phases and strictly controlled interface. The diffusion and kinetic control of the process can be distinguished by varying the stirring rate, and the extraction rate constants can be calculated by analyzing changes in the phase compositions in time. This method gives well reproducible results but is time-consuming and requires large volumes of the phases [14–16].

In the single drop method, a drop of one of the phases passes through a layer of the other phase in a column. Since the mass transfer occurs on the drop surface, the effect of hydrodynamic parameters such as the drop size and velocity and can be estimated accurately. The method allows the extraction rate data to be obtained quickly but it is sensitive to the drop formation and coalescence conditions, which can complicate the result interpretation [17–19].

The AKUFVE installation (Apparat för Kontinuerlig Utvärdering för Vätske–Vätske Extraktion) is intended for continuous measurement of the distribution ratios under conditions close to those used in industry. The system includes a temperature-controlled chamber where the phases are continuously stirred, a centrifuge for instantaneous separation, and detectors. The method allows obtaining data in real time and is suitable for studying the extraction of short-lived radionuclides. However, it requires sophisticated equipment and large amounts of reagents [20–22].

The microfluid approach is based on the interaction between the organic and aqueous phases in microchannels where the contact time, contact surface area, and flow velocity can be thoroughly controlled. Such systems allow studying very fast processes with high time resolution and minimal substance volumes. However, the use of microfluid methods requires the special technique including high-resolution microscopy and fine tuning of microfluid devices [22, 23].

The horizontal rotating vessel method consists in using a system of two cylinders in which the inner part rotates, ensuring continuous renewal of the interface. This allows high-accuracy modeling of various hydrodynamic regimes and determination of the contribution of the diffusion and chemical reactions to the overall process. The method is suitable for systems that are highly sensitive to changes in the interfacial surface area but requires accurate mechanics and design parameters [7, 24].

The approach we suggest is based on attenuated total reflection (ATR) IR spectroscopy. It is a modern analytical method for recording complexation processes directly at the interface. The IR radiation is reflected from the surface of a crystal with a high refractive index (e.g., diamond) and partially penetrates into the medium being studied. The on-line recording of the ATR IR spectra allows monitoring of changes in the intensity of absorption bands of extractant functional groups (e.g., P=O, C=O), which reflects the course of the mass transfer.

The ATR IR spectroscopy allows *in situ* monitoring of an extraction process in real time without sampling and with the minimal phase volumes. This is extremely important in operations with radionuclides when it is important to minimize the interference into the system. The method showed high efficiency in studying the extraction with both mono- and polyfunctional extractants. It also allows registration of stepwise complexation mechanisms and discrimination of the diffusion and chemical reaction contributions [25–30].

Studying the europium and yttrium extraction kinetics is of particular importance. Europium is a chemical analog of americium and curium, which makes studying its extraction very important for the development of minor actinide separation methods [31]. Yttrium-90, in

turn, is demanded by nuclear medicine, and studying its extraction recovery is required primarily for its efficient separation from the parent strontium-90 and preparation of radiopharmaceuticals with high radiochemical purity [32].

Here we apply the procedure that we developed previously for recording the ATR IR spectra [33, 34] to studying the metal extraction kinetics with mono- and polyfunctional ligands. The results are compared to those obtained using the classical Lewis diffusion cell method.

EXPERIMENTAL

Reagents and Equipment

The following chemicals were used: triamylphosphine oxide (TAPO), octyl(phenyl)-N,N-diisobutylcarbamoylmethylphosphine oxide (CMPO), N,N,N',N'-tetraoctyldiglycolamide (TODGA), diphenyl-N,N-dibutylcarbamoylmethylphosphine oxide (DPCMPO), 8-hydroxyquinoline (8-HQ), 2,3-dihydroxynaphthalene (2,3DHN), methyltrioctylammonium carbonate (MTOAC) (Khlopin Radium Institute, Russia), dichloroethane (DCE), tetrachloroethylene (TCE) (Ekos, Russia), butyl acetate (BuAc), 1-[2-bis(4-methylphenyl)phosphoryl-heptyl-(4-methylphenyl)phosphoryl]-4-methylbenzene (DiPO), $Eu(NO_3)_3 \cdot 6H_2O$, $CsNO_3$ (Vekton, Russia), and $Y_2(CO_3)_3 \cdot 5H_2O$ (Chemcraft, Russia) (Table 1).

The Fourier IR absorption spectra were recorded with a Simex FT-800 spectrometer using a Simex ATR-A attachment (Simex, Russia) with a diamond crystal (operation surface diameter 2.4 mm). The measurements were performed in the range 500–4000 cm^{-1} with 2 cm^{-1} resolution.

Solution Preparation

A 0.6 M aqueous solution of europium nitrate was prepared by dissolving a 6.69 g portion of $Eu(NO_3)_3 \cdot 6H_2O$ in a 25 mL volumetric flask. To study the kinetics of the extraction from carbonate-containing alkaline media, we prepared a 0.01 M yttrium solution containing 3 M potassium carbonate. For this purpose, we dissolved 10.37 g of K_2CO_3 in water in a 25 mL volumetric flask and added 0.089 g of $Y_2(CO_3)_3$. After the complete dissolution of the reagents, the solutions were saturated with an organic diluent (DCE or TCE)

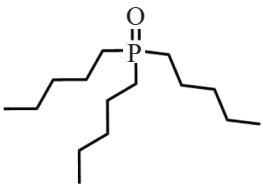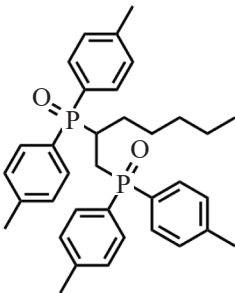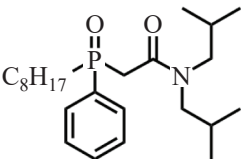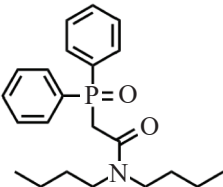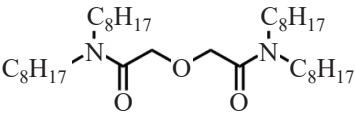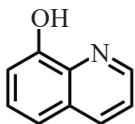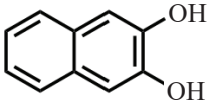by adding 0.5 mL of the organic diluent and stirring on a shaker for 10 min. Then, the solutions were centrifuged, and the aqueous phases were used for the experiments. A 0.001 M yttrium + 1 M Na_2CO_3 solution was prepared in a volumetric flask from accurately weighed portions of $Y_2(CO_3)_3$ and Na_2CO_3. The solution was saturated with BuAc at 1 : 1 ratio of the aqueous and organic phases with stirring for 10 min. The system was centrifuged, and the BuAc-saturated aqueous phase was separated and used for further experiments. A 0.01 M H_2SO_4 solution was prepared in a volumetric flask by dilution of a 0.05 M H_2SO_4 solution prepared from Fixanal (standard sample).

Solutions of organic extractants (TAPO, CMPO, DPCMPO, DiPO, 8-HQ) were prepared by dissolving a weighed portion of the extractant in DCE. A 0.01 M 2,3DHN + 0.015 M MTOAC solution in BuAc was prepared from the accurately weighed portions of the extractants and was stirred for 12 h until it became dark violet. A 0.6 M TODGA solution was prepared by dissolving the weighed portion in TCE because the density of the solution of TODGA in DCE was lower than that of the $Eu(NO_3)_3$ solution, which would make it impossible to study the extraction kinetics by ATR IR spectroscopy. All the organic solutions after their separation were saturated with water by adding 0.5 mL of distilled water and stirring on a shaker for 10 min. Then, the solutions were centrifuged, and the organic phases were used in the experiments.

ATR IR Study of Extraction Kinetics

The spectra were measured in the range 500–3500 cm^{-1} with 2 cm^{-1} resolution. The interval between recording the spectra was 3 s. The kinetic experiments were performed in a microcell in the form of a polypropylene tube (d = 4, 6, or 8 mm) with a hole in the upper lateral part for introducing liquid samples (Fig. 1a). The samples were introduced with 25- and 50-µL chromatographic syringes or a 100-µL dosing syringe. First, the organic phase (extractant solution) was added, and the initial spectrum was recorded. Then, the aqueous phase was added, and the spectra were recorded at 3- or 10-s intervals. The spectra were recorded until no changes were observed at characteristic wavelengths in four or five successive scans. When performing the experiments, the microcell was arranged so that the cell material did not contact the ATR crystal and was pressed to the ATR attachment to reduce the liquid evaporation.

Table 1. Extraction systems and fission products extracted with them

No.	Cation	Extraction system	Structural formula of extractant
1	Eu^{3+}	Triamylphosphine oxide (TAPO) in dichloroethane	
2		1-[2-Bis(4-methylphenyl)phosphorylheptyl-(4-methylphenyl)phosphoryl]-4-methylbenzene (DiPO) in dichloroethane	
3		Octylphenyl(N,N-diisobutylcarbamoylmethyl)phosphine oxide (CMPO) in dichloroethane	
4		Diphenyl(N,N-dibutylcarbamoylmethyl)phosphine oxide (DPCMPO) in dichloroethane	
5		N,N,N',N'-Tetraoctyldiglycolamide (TODGA) in tetrachloroethylene	
6	Y^{3+}	8-Hydroxyquinoline (8-HQ) in dichloroethane	
7		2,3-Dihydroxynaphthalene (2,3DHN) in butyl acetate	

The membrane extraction was studied using a modified Lewis cell (Fig. 1b). All the three phases were stirred with a magnetic stirrer, and the membrane phase was stirred using a floating magnetic anchor. The phase stirring was tuned in the same fashion as for the classical Lewis cell. The volume of each phase in studying the membrane extraction was 12 mL, and the interfacial surface area was 3.14 cm². Aqueous phase samples (50 μL each) were taken with a 100 μL dosing syringe. The samples were diluted by a factor of 2500 with a 0.1 M
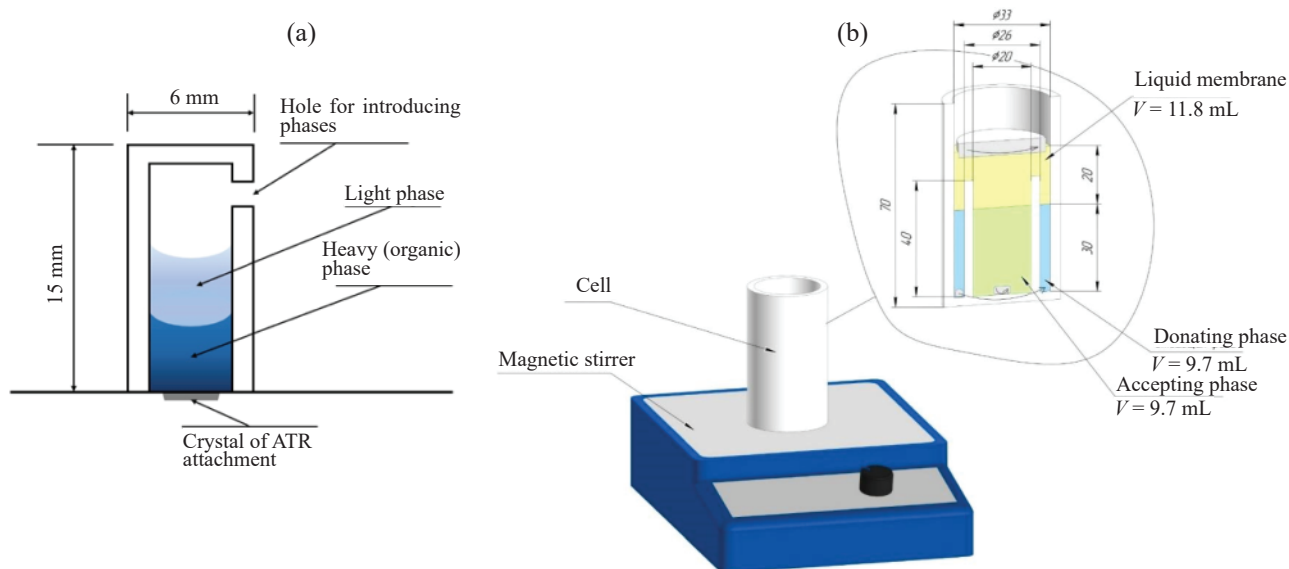
(a)

(b)

Fig. 1. (a) Scheme of the microcell for studying the extraction kinetics by ATR IR [33]; (b) modified Lewis cell for studying the membrane extraction kinetics.

HNO$_3$ solution and were then analyzed by inductively coupled plasma atomic emission spectrometry.

Kinetics Determination by Classical and Membrane Extraction with a Lewis Cell

A Lewis cell was fabricated for studying the extraction kinetics by the classical method. To this end, a 50-mL volumetric vial was truncated to a volume of 25 mL. The organic (heavy) phase was stirred with a magnetic stirrer, and the aqueous (light) phase, with an overhead stirrer. The phase stirring was tuned so as to be maximally vigorous but without disturbing the interface surface integrity. The volume of each phase in studying the extraction in a Lewis cell was 10 mL. The samples were taken from the aqueous phase with a 100-μL dosing syringe. The volume of each sample was 50 μL. The samples were diluted by a factor of 2500 with a 0.1 M HNO$_3$ solution and were then analyzed by inductively coupled plasma atomic emission spectroscopy. To obtain the kinetic curves of the yttrium extraction with a mixture of 2,3DHN and MTOAC in the classical Lewis cell, we brought in contact 8-mL portions of the aqueous and organic phases, took their samples of equal volume at definite intervals, and determined their yttrium content. The interfacial surface area was 10.2 cm^2.

The metal concentrations in the aqueous phase in the kinetic experiments with the Lewis cell were measured by an ICPE-9000 inductively coupled plasma optical emission spectrometer (Shimadzu, Japan).

Calorimetric Study of the Extraction

Calorimetric studies of mixing were performed with a Setaram C80 Calvet calorimeter (Setaram, France). To study the CMPO–Eu system, 1 mL of a 0.1 M solution of CMPO in DCE and 2 mL of a 0.1 M aqueous Eu(NO$_3$)$_3$ solution were added into the calorimeter cell. The solutions were separated from each other with an aluminum foil. Immediately after placing the cell with the solutions into the calorimeter, the recording of the thermal effects in the system was switched on. After the attainment of the thermal equilibrium in the system, the aluminum foil was broken with a striker, and the stirring was switched on. When thermal equilibrium was attained, a blank sample (without extractant) was pierced with a buoy after the test sample and the thermal effect was also determined in it to take into account the effect of solution mixing.

RESULTS AND DISCUSSION

Extraction System 0.6 M TAPO in Dichloroethane–0.6 M Eu(NO$_3$)$_3$

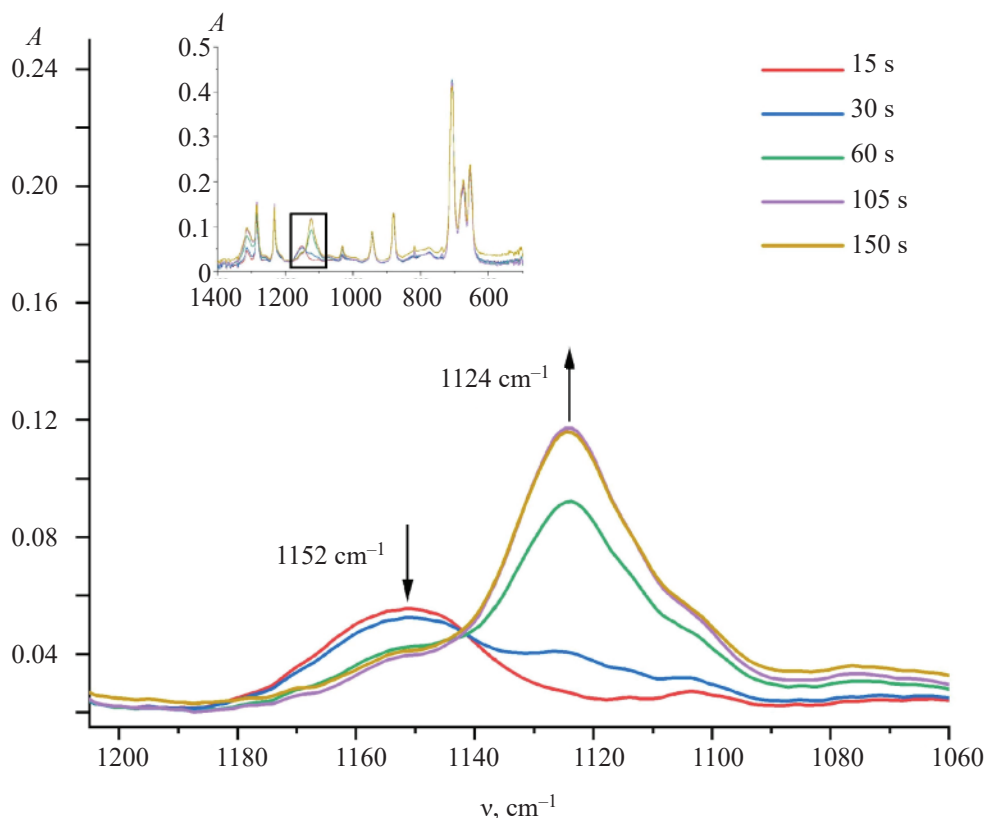The IR spectra of the organic phase in the extraction of Eu^{3+} with a solution of TAPO in DCE at phase

Fig. 2. Evolution of the IR spectra (range of $\nu_{P=O}$ stretching vibration bands) of the organic phase in the course of Eu^{3+} extraction with a solution of TAPO in DCE.

volumes of 10 μL were recorded for 150 s. The most pronounced changes occur in the range 1200–1080 cm^{-1}. This range includes the stretching vibration band $\nu_{P=O}$ of free TAPO molecules at 1152 cm^{-1}. Its intensity decreases with an increase in the phase contact time. In addition, with the start of the extraction, the stretching vibration band $\nu_{P=O}$ of TAPO solvates with the Eu^{3+} ion appears in this range at 1124 cm^{-1} (Fig. 2).

Based on the IR spectra of the Eu^{3+}–TAPO system, the kinetic curves were plotted in the reduced coordinates $(A - A_0)/(A_{max} - A_0)$ vs. t (Fig. 3).

The extraction kinetics can be described similarly to the description of a reversible first-order reaction when the distribution ratios are not very high. However, as seen from the plot, the kinetic curves for the Eu^{3+}–TAPO system correspond rather to curves for successive reactions. Up to the 65th second, the extraction rate increases, which can be attributed to the TAPO accumulation at the interphase boundary due to its surface activity or to the diffusion of TAPO solvates with the Eu^{3+} ion from the interface to the surface of the ATR crystal. Af-

ter the 65th second, the extraction rate can be described similarly to the rate of a reversible first-order reaction.

To reveal causes of the "abnormal" shape of the extraction kinetic curve, we performed experiments on
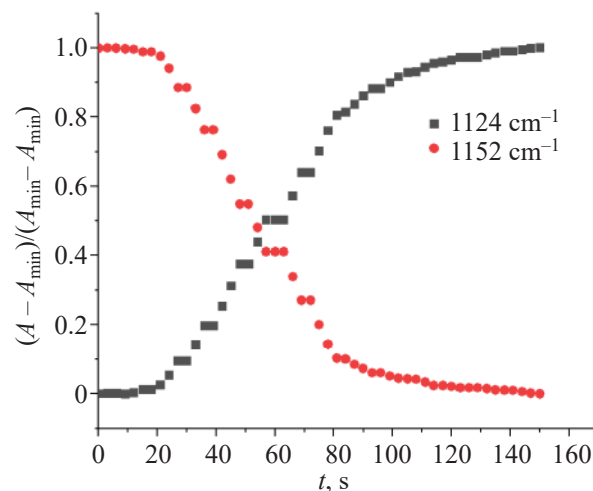

Fig. 3. Kinetic curves of the Eu^{3+} extraction with a solution of TAPO in DCE, based on a series of IR spectra.
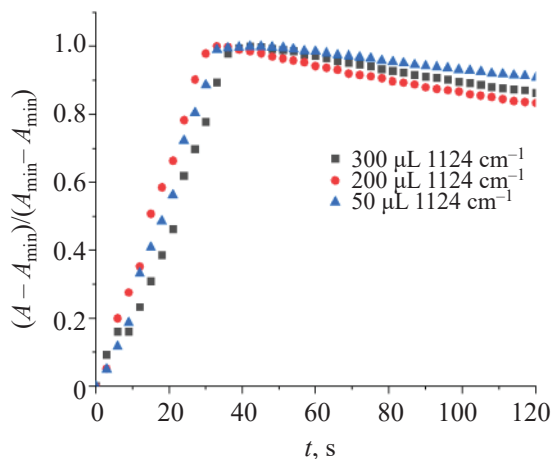
Fig. 4. Kinetic curves of the diffusion of TAPO solvates with Eu^{3+} ions in a solution of TAPO in DCE, based on a series of IR spectra.

the diffusion of Eu^{3+}–TAPO solvates in the bulk of the organic phase depending on the organic phase volume (layer height). The results are presented in Table 2 and Fig. 4.

The data obtained show that the diffusion of TAPO solvates with Eu^{3+} ions occurs, on the average, within approximately 30 s at the organic phase volume larger than 50 μL, after which the peak intensity starts to decrease owing to the dichloroethane evaporation (because there is no upper aqueous layer decelerating the evaporation). Therefore, we interpreted the kinetic curve in Fig. 3 as corresponding to two successive reactions A → B → C, where the reaction A → B is the formation of TAPO solvates with Eu^{3+} ions and the reaction B → C is the diffusion of the solvates from the surface layer to the ATR crystal surface. To reduce the effect of diffusion in studying the extraction kinetics, we decided to use minimum possible volumes of the organic and aqueous phases. We performed an additional kinetic experiment at TAPO and Eu^{3+} solution volumes of 10 μL and calculated the extraction rate constant: $k = 3.3 \times 10^{-4}$ cm s^{-1}.

To check the results obtained, we fabricated a Lewis

Table 2. Results of experiments on the diffusion of TAPO solvates with the Eu^{3+} ion in the organic phase

Volume, μL	Liquid layer height	Diffusion time, s
50	2	33
200	8	39
300	12	42

diffusion cell used to the extraction kinetics. For this purpose, we prepared 0.3 M solutions of Eu(NO$_3$)$_3$ and TAPO by dilution of the 0.6 M solutions. 10 mL of the extractant solution was added into the Lewis cell with a dosing syringe, than 10 mL of the Eu(NO$_3$)$_3$ solution was carefully added so as to avoid mixing of the phases and emulsion formation. The stirring rate was chosen in such a way not to change the phase boundary in the course of the experiment. From the data obtained, we plotted the kinetic curve and calculated the extraction rate constant. It agreed with the previously obtained data ($k = 3.3 \times 10^{-4}$ cm s^{-1}) and published data for the analogous Nd^{3+}–TOPO system ($k = 4.8 \times 10^{-4}$ cm s^{-1}) [35].

Thus, we have demonstrated by the example of studying the extraction kinetics in the system with TAPO that ATR IR spectroscopy [33, 34] and the method based on the Lewis cell give close rate constants, but the ATR IR advantages are much shorter experiment time (150 instead of 1800 s) and much smaller volumes of phases (10 instead of 10000 μL).

Extraction System 0.6 M DiPO in Dichloroethane–0.6 M Eu(NO$_3$)$_3$

DiPO as an extractant with two PO groups was chosen for checking the suitability of ATR IR spectroscopy for studying the kinetics of the metal extraction with polyfunctional ligands forming chelate complexes. The experiments were performed in the middle-size cell ($d = 6$ mm) with 50-μL portions of 0.6 M solutions of DiPO in DCE and of Eu(NO$_3$)$_3$. Figure 5 shows the spectra in the range 1210–1110 cm^{-1}.

This range includes the stretching vibration band $\nu_{P=O}$ of free DiPO molecules at 1178 cm^{-1}, whose intensity decreases with an increase in the phase contact time, and the stretching vibration band $\nu_{P=O}$ of DiPO solvates with the Eu^{3+} ion at 1143 cm^{-1}. The kinetic curve based on the data obtained was constructed, and the rate constant was calculated.

The shape of the kinetic curve suggests that, as in the system with TAPO, the diffusion also strongly influences the process, which is manifested in the presence of an inflection point. The ascent of the kinetic curve for the wavenumber of 1178 cm^{-1} is due to the superposition of the peaks originating from the free extractant molecules and from the solvates at equilibrium. A study of the extraction kinetics in this system shows that ATR IR spectroscopy is an efficient tool for systems with both
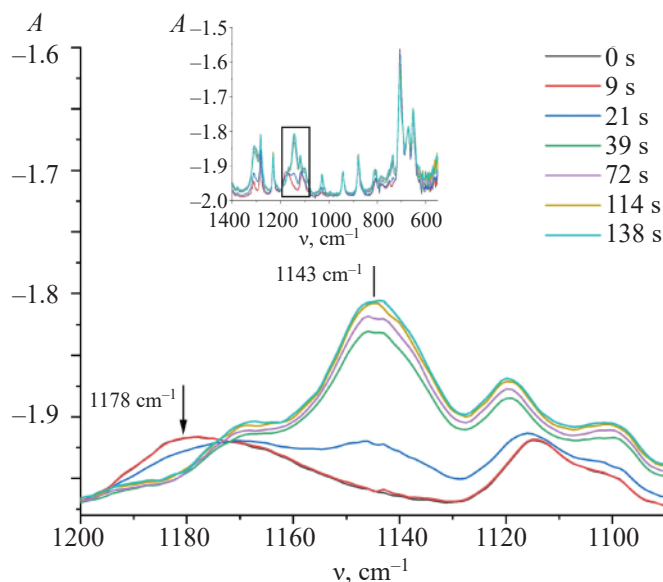
Fig. 5. Evolution of the IR spectra (range of $\nu_{P=O}$ stretching vibrations) of the organic phase in the course of Eu^{3+} extraction with a solution of DiPO in DCE.

polyfunctional ligands and ligands containing several identical functional groups.

Extraction System 0.6 M CMPO in Dichloroethane–0.6 M Eu(NO₃)₃

CMPO as an extractant with PO and CO groups, exhibiting high performance in the recovery of rare earth metals [36, 37], was chosen to check the ability of ATR IR spectroscopy to register evolution with time of absorption bands belonging to different functional groups of the extractant. We chose the ranges $1220–1080\ cm^{-1}$ for the PO group and $1660–1570\ cm^{-1}$ for the CO group. The experiments were performed in the middle-size cell ($d = 6$ mm) with 50-μL portions of 0.6 M solutions of CMPO and $Eu(NO_3)_3$. Figure 6a shows the evolution of the IR spectra (region of $\nu_{P=O}$ stretching vibrations) of the organic phase in the course of Eu^{3+} extraction with a solution of CMPO in DCE.

This range of the spectrum includes the stretching vibration band $\nu_{P=O}$ of free CMPO molecules at $1194\ cm^{-1}$, whose intensity decreases with an increase in the phase
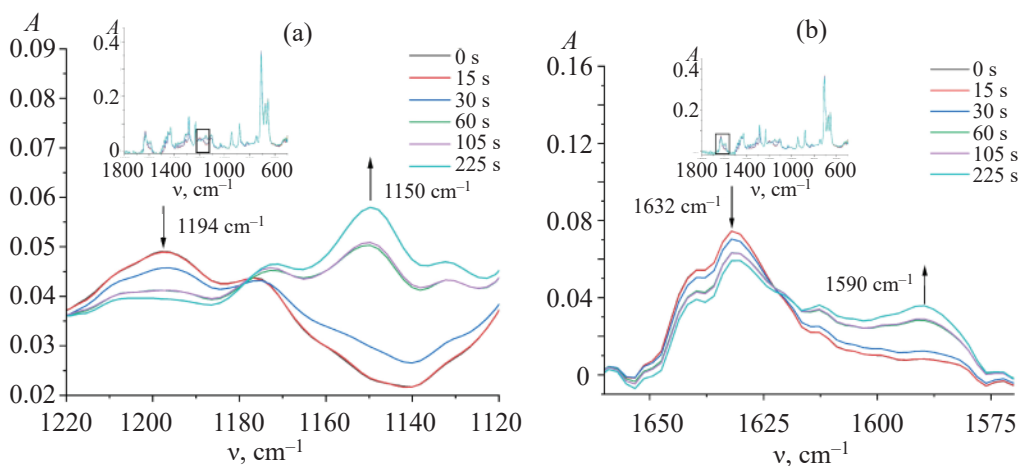

Fig. 6. Evolution of the IR spectra (ranges of (a) $\nu_{P=O}$ and (b) $\nu_{C=O}$ stretching vibrations) of the organic phase in the course of Eu^{3+} extraction with a solution of CMPO and DCE.
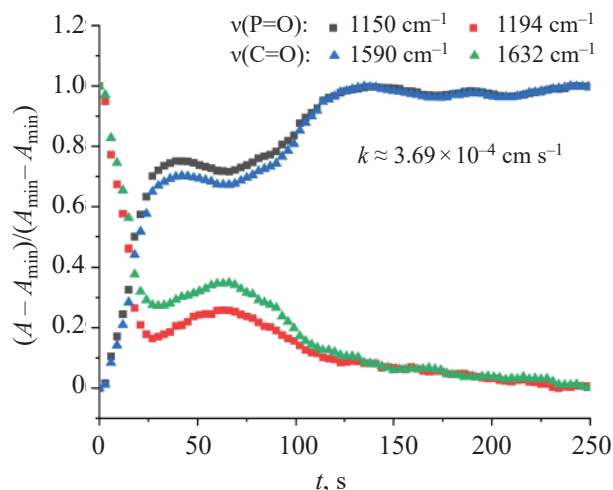
Fig. 7. Kinetic curves of the Eu^{3+} extraction with a solution of CMPO in DCE, based on a series of IR spectra.

contact time, and the band at 1150 cm^{-1}, belonging to stretching vibrations of coordinated P=O groups in solvates of the extractant with the Eu^{3+} ion. We also considered the range 1660–1570 cm^{-1} (Fig. 6b) containing the stretching vibration band $\nu_{C=O}$ of C=O groups that are not coordinated to the metal ion (1632 cm^{-1}), whose intensity decreases as a result of formation of solvates with Eu^{3+} ions, and the band at 1590 cm^{-1}, belonging to the stretching vibrations of CMPO C=O groups coordinated to Eu^{3+} ions.

The kinetic curves based on our experimental data are shown in Fig. 7.

The band corresponding to the coordination of CMPO molecules to europium via P=O bond increases in the initial period of the extraction more rapidly than does the band corresponding to the CMPO coordination via C=O bond. After that, the equilibrium is attained. The presence of two steps in the kinetic curves can be attributed to successive coordination of Eu^{3+} ions via P=O and C=O bonds to form a chelate (Fig. 8). As the intensity of the band at 1150 cm^{-1} increases faster than
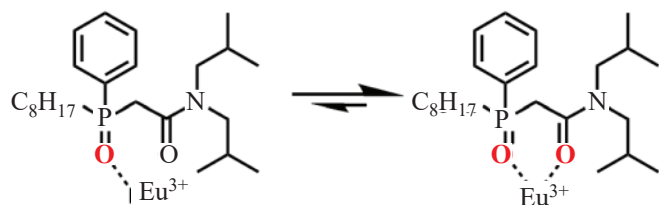

Fig. 8. Coordination and chelation of Eu^{3+} with CMPO.

does that of the band at 1590 cm^{-1} in the initial period of extraction, it can be assumed that the major fraction of Eu^{3+} ions are primarily coordinated via P=O bond in CMPO.

The concept of stepwise chelate formation in the course of extraction is confirmed by published data [30, 38, 39]. To prove experimentally the stepwise complexation, the system with CMPO was studied by calorimetry. The exothermic effect caused by the Eu^{3+} complexation with CMPO also consists of two steps, supporting the stepwise chelation concept. The enthalpy of complexation, determined after subtracting the enthalpy of mixing determined in the blank experiment, is –24.6 kJ/mol, which well agrees with the published data [40].

Extraction System 0.6 M DPCMPO in Dichloroethane–0.6 M Eu(NO₃)₃

To study the possible stepwise complexation mechanism in more detail, we performed an experiment with another extractant containing two different functional groups, DPCMPO. The experiments were carried out in the middle-size cell (d = 6 mm) with 50-μL portions of 0.6 M solutions of DPCMPO and Eu(NO$_3$)$_3$. As in the system with CMPO, we chose two ranges of the spectrum. The range 1220–1110 cm^{-1} includes the stretching vibration band $\nu_{P=O}$ of free DPCMPO molecules at 1198 cm^{-1} and the band at 1163 cm^{-1}, belonging to stretching vibrations of P=O groups coordinated to europium. The range 1670–1560 cm^{-1} includes the stretching vibration band $\nu_{C=O}$ of free extractant molecules at 1637 cm^{-1} and the band at 1597 cm^{-1}, belonging to stretching vibrations of C=O groups coordinated to Eu^{3+} ions.

As in the case with CMPO, there are two steps in the kinetic curves. However, with DPCMPO there is no difference in the rate of the growth of the peaks corresponding to the Eu^{3+} coordination via P=O and C=O bonds. This may be due to the fact that the equilibrium in the system with DPCMPO is attained two times faster than in the system with CMPO. Hence, the chelation of DPCMPO with Eu^{3+} ions also proceeds faster than in the system with CMPO, and the difference between the P=O and C=O coordination rates cannot be revealed by IR spectroscopy. This is confirmed by the calculated extraction rate constants: 3.69 × 10^{-4} cm s^{-1} for the system with CMPO and 11.1 × 10^{-4} cm s^{-1} for the system with DPCMPO.
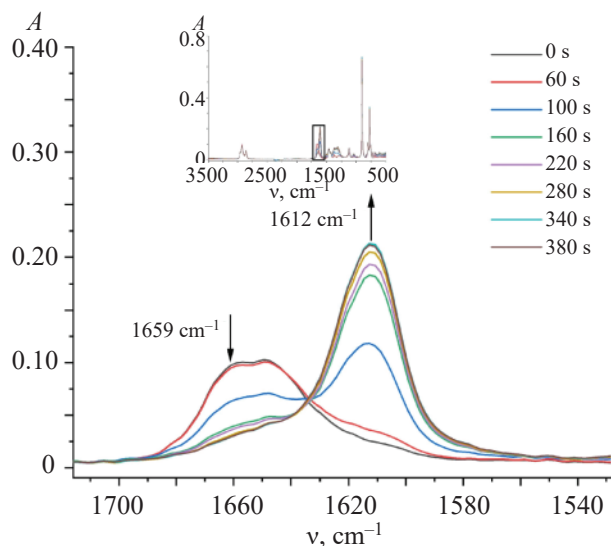
Fig. 9. Evolution of the IR spectra in the region of $\nu_{C=O}$ stretching vibrations in the course of Eu^{3+} extraction with a solution of TODGA in TCE.

*Extraction System 0.6 M TODGA
in Tetrachloroethylene–0.6 M Eu(NO$_3$)$_3$*

The extraction kinetics was also studied for the system with a chelating extractant containing two C=O groups (TODGA). The experiments were performed in the middle-size cell ($d = 6$ mm) with 50-μL portions of 0.6 M solutions of TODGA in TCE (TCE was taken because the density of the 0.6 M solution of TODGA in DCE was lower than that of the Eu(NO$_3$)$_3$ solution) and Eu(NO$_3$)$_3$. We chose the range 1710–1530 cm^{-1} (Fig. 9). It includes the stretching vibration band $\nu_{C=O}$ of C=O groups not involved in the coordination to Eu^{3+} (1659 cm^{-1}), whose intensity decreases in the course of the experiment, and the $\nu_{C=O}$ band at 1612 cm^{-1}, corresponding to C=O stretching vibrations in TODGA solvates with Eu^{3+} ions. No changes in the course of the Eu^{3+} extraction were observed in the region of 1120 cm^{-1}, corresponding to C–O–C stretching vibrations. This fact

confirms that the ether oxygen atom is not involved in the complexation.

There are two well-defined steps in the kinetic curves, attributable to the chelate formation (Fig. 10). That is, the chelate can be formed stepwise also in systems with symmetrical extractants containing identical functional groups.

Analysis of the kinetic curves and rate constants shows that the extraction rate with the monofunctional extractant (TAPO) ($k = 3.3 \times 10^{-4}$ cm s^{-1}) is lower than with the polyfunctional extractants. This may be associated with the presence of several coordination sites in polyfunctional extractants and with the formation of more stable chelates. The extraction rate is also influenced by the structure of the polyfunctional extractant: DPCMPO extracts europium three times faster ($k = 1.1 \times 10^{-3}$ cm s^{-1}) than CMPO does ($k = 3.7 \times 10^{-4}$). This can be attributed to smaller number of possible conformations of the P(Ph)$_2$ fragment compared to P(C$_8$H$_{17}$)(Ph) and hence to faster conformational adaptation of the extractant molecule for the chelation.

*Extraction System 0.1 M 8-HQ
in Dichloroethane–0.01 M Y$_2$(CO$_3$)$_3$*

Carbonate media were chosen owing to their ability to efficiently retain strontium with the simultaneous conversion of yttrium to a soluble form suitable for the subsequent extraction. Because the solubility of Y$_2$(CO$_3$)$_3$ in water is extremely low, for the yttrium carbonate dissolution we preliminarily prepared a 3 M K$_2$CO$_3$ solution and then dissolved yttrium carbonate in it [41, 42]. We prepared a 0.01 M aqueous solution of Y$_2$(CO$_3$)$_3$ and a 0.1 M solution of 8-HQ in DCE. We recorded the spectra of a 0.1 M solution of 8-HQ in DCE and of the 8-HQ solution after the extraction. The extraction was performed by stirring 0.5-mL portions of a 0.01 M yttrium solution and a 0.1 M 8-HQ solution for 4 h at 25°C. Since no apparent changes were observed in
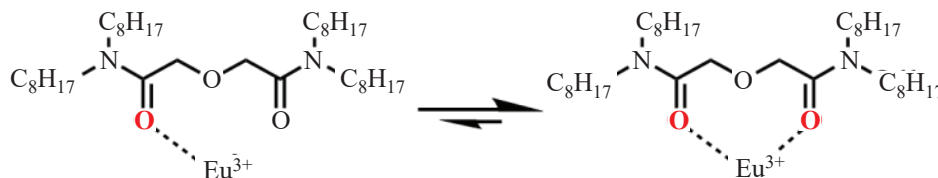

Fig. 10. Coordination and chelation of Eu^{3+} with TODGA.
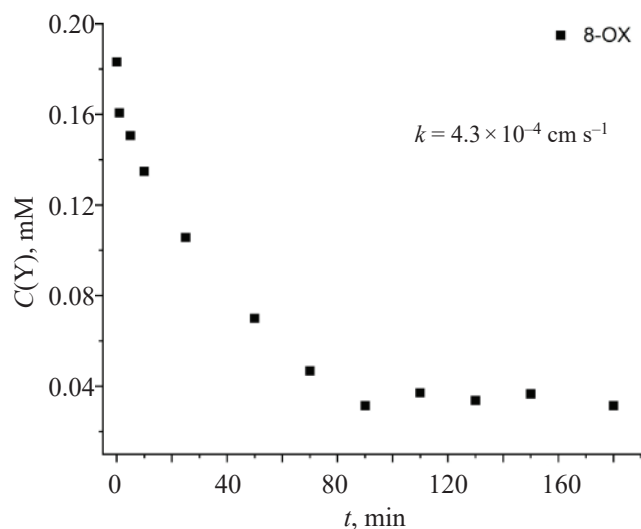
Fig. 11. Extraction kinetic curve for the system 0.1 M 8-HQ in dichloroethane–0.01 M $Y_2(CO_3)_3$, obtained using the Lewis cell.

the spectra before and after the extraction, we assumed that the yttrium concentration was insufficient for studying the extraction kinetics in this system by ATR IR spectroscopy. The kinetics was studied using the Lewis cell (Fig. 11).

Extraction System 0.01 M 2,3DHN + 0.015 M MTOAC
in Butyl Acetate–0.001 M $Y_2(CO_3)_3$

As shown previously, 2,3-dihydroxynaphthalene (2,3DHN) in combination with methyltrioctylammo-

nium carbonate (MTOAC) efficiently extracts yttrium from carbonate solutions [43]. However, no kinetic data are available for this system. We have studied the kinetics of the yttrium extraction from a 1 M sodium carbonate solution with a synergistic mixture of 2,3DHN and MTOAC in butyl acetate and of the yttrium stripping from the equilibrium organic phase with 0.01 M H_2SO_4 in the classical two-phase Lewis cell and the kinetics of the yttrium mass transfer in the modified three-phase cell to evaluate the characteristics of the membrane extraction. The kinetic curves are shown in Fig. 12.

The extraction kinetics corresponds to a reversible first-order reaction. The rate constant of the yttrium extraction with a mixture of 2,3DHN and MTOAC, calculated from the kinetic curve ($k = 1.5 \times 10^{-3}$ cm s^{-1}), is higher by an order of magnitude than that obtained previously for 8-hydroxyquinoline ($k = 4.3 \times 10^{-4}$ cm s^{-1}). Such an increase in the rate constant can be primarily caused by the synergistic effect of the 2,3DHN–MTOAC mixture, consisting in the preliminary deprotonation of 2,3DHN hydroxy groups with MTOAC carbonate ion in butyl acetate.

The kinetics of the yttrium mass transfer was studied in the cell with a free liquid membrane. Simultaneously, we monitored the yttrium content in the donating and accepting phases and the proton concentration in the accepting phase. The theoretical kinetic curve was calculated taking into account the extraction rate constant determined using the Lewis cell, taking into account the
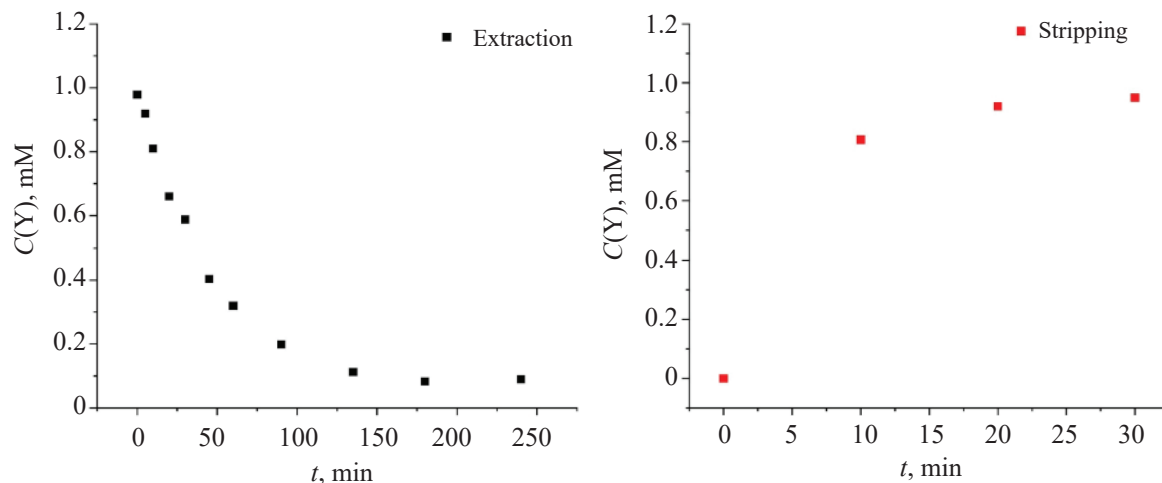

Fig. 12. Kinetic curves of the yttrium extraction in the 2,3DHN + MTOAC in BuAc–$Y_2(CO_3)_3$ system and of the yttrium stripping with 0.01 M H_2SO_4, obtained using the Lewis cell. $C(Y)_{init} = 0.001$ M, $C(2,3DHN) = 0.01$ M, and $C(MTOAC) = 0.015$ M.
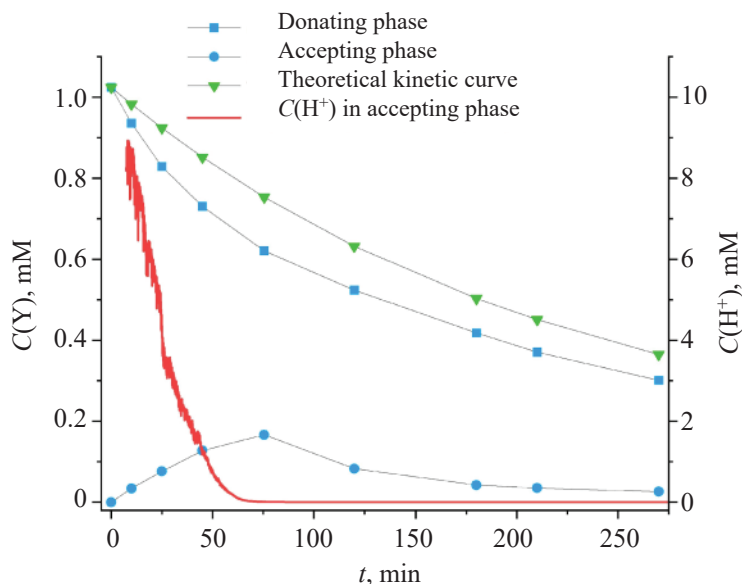
Fig. 13. Stripping kinetic curves for the system consisting of 2,3DHN + MTOAC in BuAc, $Y_2(CO_3)_3$, and H_2SO_4; $C(Y)_{nit} = 0.001$ M, $C(2,3DHN) = 0.01$ M, $C(MTOAC) = 0.015$ M, and $C(H_2SO_4) = 0.01$ M.

interface surface area in the cell with a free liquid membrane (Fig. 13).

In the system chosen for the study, the yttrium stripping is accompanied by the proton transfer from the accepting phase to the donating phase. Complete neutralization of H_2SO_4 is observed, after which the yttrium stripping ceases and yttrium starts to be concentrated in the membrane phase. Up to the neutralization of the accepting aqueous phase, the yttrium mass transfer proceeds faster than it follows from the calculations. Then, the difference between the theoretical and experimental kinetic curves becomes constant. High rate of the membrane process compared to the classical extraction is due to the irreversibility of the metal transfer from the membrane to the accepting phase.

CONCLUSIONS

A study of the kinetics of the europium and yttrium extraction with mono- and polyfunctional ligands by ATR IR spectroscopy and with a Lewis diffusion cell revealed some features of the extraction in the systems Eu^{3+}–TAPO, Eu^{3+}–DiPO, Eu^{3+}–CMPO, Eu^{3+}–DPCMPO, Eu^{3+}–TODGA, Y^{3+}–8-HQ, and Y^{3+}–2,3DHN. The extraction rate can be influenced by the diffusion of metal–extractant solvates in the extractant solution to the ATR surface, the solvate formation mechanism, and the kind of the extractant.

For the systems with Eu^{3+}, the extraction rate with monofunctional TAPO is lower (3.3×10^{-4} cm s^{-1}) than with chelating extractants (DPCMPO, 1.1×10^{-3} cm s^{-1}), which is caused by the presence of a large number of active sites in the latter case. In the series of chelating ligands, the structure of the molecule becomes significant: DPCMPO extracts europium 3 times faster ($k = 1.1 \times 10^{-3}$ cm s^{-1}) than CMPO does ($k = 3.7 \times 10^{-4}$). This can be attributed to the smaller number of conformations of the $P(Ph)_2$ fragment compared to $P(C_8H_{17})$ (Ph) and to the high rate of the conformational adaptation of the molecule for the chelation. A stepwise chelation mechanism was revealed for the polyfunctional extractants. It was indirectly confirmed by the calorimetric titration (double-peak shape of the exothermic effect of the reaction).

For the systems with Y^{3+}, the extraction rate constants were calculated for 8-hydroxyquinoline and for the mixed extractant (2,3DHN and MTOAC). Higher rate constants in the case of the mixed extractant ($k = 1.5 \times 10^{-3}$ cm s^{-1}), compared to 8-hydroxyquinoline ($k = 4.3 \times 10^{-4}$ cm s^{-1}), can be attributed to the synergistic effect consisting in the deprotonation of the 2,3DHN hydroxy groups with MTOAC carbonate ion in butyl acetate.

A study of the yttrium mass transfer kinetics in the cell with a free liquid membrane shows that the yttrium mass transfer proceeds faster than follows from the cal-

culation until neutralization of the accepting aqueous phase. After that, the difference between the experimental data and calculation results becomes constant.

CONFLICT OF INTEREST

The authors declare that they have no conflicts of interest.

REFERENCES

1. Mincher, B.J., Modolo, G., and Mezyk, S.P., *Solvent Extr. Ion Exch.,* 2009, vol. 27, no. 1, pp. 1–25.

2. Danesi, P.R. and Chiarizia, R., *CRC Crit. Rev. Anal. Chem.,* 1980, vol. 10, no. 1.

3. Holder, J.V., *Radiochim. Acta,* 1978, vol. 25, nos. 3–4, pp. 171–180.

4. Gindin, L.M., *Ekstraktsionnye protsessy i ikh primenenie* (Extraction Processes and Their Use), Moscow: Atomizdat, 1984.

5. Paiva, A.P. and Malik, P., *J. Radioanal. Nucl. Chem.,* 2004, vol. 261, pp. 485–496.

6. Herbst, R.S., Baron, P., and Nilsson, M., in *Advanced Separation Techniques for Nuclear Fuel Reprocessing and Radioactive Waste Treatment,* Cambridge: Woodhead, 2011, pp. 141–175.

7. El-Hefny, N.E., *J. Phys. Sci.,* 2017, vol. 28, no. 1, p. 129.

8. Danesi, P.R., in *Solvent Extraction Principles and Practice, Revised and Expanded*, CRC, 2004, pp. 218–268.

9. Fomin, V.V., *Kinetika ekstraktsii* (Extraction Kinetics), Moscow: Atomizdat, 1978.

10. Nanda, A.K. and Sharma, M.M., *Chem. Eng. Sci.,* 1966, vol. 21, no. 8, pp. 707–713.

11. Konopkina, E.A., Gopin, A.V., and Matveev, P.I., *J. Mol. Liq.,* 2024, article 126025.

12. Retegan, T., van den Hoven, K.W.J.C., van der Merwe, F.J., and van der Merweet, M.J.M., *Solvent Extr. Ion Exch.,* 2014, vol. 32, no. 7, pp. 720–736.

13. Hill, C., Guillaneux, D., Berthon, L., and Madic, C., *J. Nucl. Sci. Technol.,* 2002, vol. 39, suppl. 3, pp. 309–312.

14. Yang, X., Wang, X., Wei, C., Zheng, S., Sun, Q., and Wang, D., *Hydrometallurgy,* 2013, vols. 131–132, pp. 34–39.

15. Danesi, P.R. and Cianetti, C., *Sep. Sci. Technol.,* 1982, vol. 17, no. 7, pp. 969–984.

16. Wang, X., Meng, S., and Li, D., *Sep. Purif. Technol.,* 2010, vol. 71, no. 1, pp. 50–55.

17. Baumgaertner, F. and Finsterwalder, L., *J. Phys. Chem.,* 1970, vol. 74, no. 1, pp. 108–112.

18. El-Hefny, N.E. and El-Dessouky, S.I., *J. Chem. Technol. Biotechnol.,* 2006, vol. 81, no. 3, pp. 394–400.

19. Cao, W., Huang, K., Wang, X., and Liuet, H., *J. Rare Earths,* 2021, vol. 39, no. 10, pp. 1264–1272.

20. Rydberg, J., Burger, W., Nygren, M., Smidsrød, O., Lindberg, A.A., Jansen, G., Lamm, B., and Samuelsson, B., *Acta Chem. Scand.,* 1969, vol. 23, pp. 647–659.

21. Chen, Z. and Wang, Y., *Chin. J. Chem. Eng.,* 2018, vol. 26, no. 2, pp. 317–321.

22. Konopkina, E.A., Gopin, A.V., Pozdeev, A.S., Chernysheva, M.G., Kalle, P., Pavlova, E.A., Kalmykov, S.N., Petrov, V.G., Borisova, N.A., Guda, A.A., and Matveev, P.I., *Phys. Chem. Chem. Phys.,* 2024, vol. 26, no. 3, pp. 2548–2559.

23. Launiere, C.A. and Gelis, A.V., *Ind. Eng. Chem. Res.,* 2016, vol. 55, no. 7, pp. 2272–2276.

24. Bromley, M.A. and Boxall, C., *Nukleonika,* 2015, vol. 60, pp. 859–864.

25. Smirnova, N.N. and Chukhlanov, V.Yu., *Infrakrasnaya spektroskopiya v khimii vysokomolekulyarnykh soedinenii: uchebnoe posobie* (Infrared Spectroscopy in the Chemistry of Macromolecular Compounds: Textbook), 2021.

26. Yaman, N. and Durakli Velioglu, S., *Foods,* 2019, vol. 8, no. 7, p. 231.

27. Parikh, S.J., Lafferty, B.J., and Sparks, D.L., *J. Colloid Interface Sci.,* 2008, vol. 320, no. 1, pp. 177–185.

28. Pintar, A., Batista, J., and Levec, J., *Analyst,* 2002, vol. 127, no. 11, pp. 1535–1540.

29. Shpachenko, I.G., Brandt, N.N., and Chikishev, A.Yu., *Vestn. Mosk. Univ., Ser. 3: Fiz. Astron.,* 2018, no. 6, pp. 67–73.

30. Tiernan, H., Byrne, B., and Kazarian, S.G., *Spectrochim. Acta, Part A: Mol. Biomol. Spectrosc.,* 2020, vol. 241, ID 118636.

31. Ansari, S.A., Pathak, P., Mohapatra, P.K., and Manchanda, V.K., *Chem. Rev.,* 2012, vol. 112, no. 3, pp. 1751–1772.

32. Lakshmanan, V.I. and Vijayan, S., in *Extraction 2018: Proc. 1st Global Conf. on Extractive Metallurgy,* Springer, 2018, pp. 1913–1930.

33. Aleksandrov, T.S., Timoshenko, V.V., Brechalov, A.A., and Smirnov, I.V., *Radiochemistry,* 2023, vol. 65, no. 2, pp. 226–229.

34. Smirnov, I.V., Karavan, M.D., Aleksandrov, T.S., Brechalov, A.A., Babitova, E.S., Timoshenko, V.V., and Ermolenko, Yu.E., *J. Radioanal. Nucl. Chem.,* 2025, vol. 334, no. 4, pp. 2729–2739.

35. El-Hefny, N.E., *Chem. Eng. Process. Process Intensif.,* 2007, vol. 46, no. 7, pp. 623–629.

36. Myasoedov, B.F., Chmutova, M.K., Kochetkova, N.E., Koiro, O.E., Pribylova, G.A., Nesterova, N.P., Medved, T.Ya., and Kabachnik, M.I., *Solvent Extr. Ion Exch.,* 1986, vol. 4, no. 1, pp. 61–81.

37. Myasoedov, B.F., Chmutova, M.K., Litvina, M.N., and Kulyako, Yu.M., *Russ. Chem. Bull.,* 1998, vol. 47, pp. 1690–1696.

38. Perez-Benito, J.F. and Nicolas-Rivases, J., *Int. J. Chem. Kinet.,* 2018, vol. 50, no. 8, pp. 591–603.

39. Dholakia, S., Gillard, R.D., and Wimmer, F.L., *Inorg. Chim. Acta,* 1982, vol. 65, p. L203.

40. Hosseinnejad, T. and Kazemi, T., *Radiochim. Acta,* 2016, vol. 104, no. 2, pp. 97–105.

41. De Vasconcellos, M.E., da Rocha, S.M.R., Pedreira, W.R., Queiroz, C.A. da S., and Abrãoet, A., *J. Alloys Compd.,* 2006, vol. 418, nos. 1–2, pp. 200–203.

42. Ryabchikov, D.I. and Ryabukhin, V.A., *Prog. Sci. Technol. Rare Earths,* 1964, vol. 1, pp. 399–415.

43. Harb, A.H.A., Balantsev, I.V., Karavan, M.D., Smirnov, I.V., and Aleksandrov, T.S., *Radiochemistry,* 2023, vol. 65, no. 2, pp. 219–225.

44. Harb, A.H.A., Balantsev, I.V., Karavan, M.D., and Smirnov, I.V., *J. Radioanal. Nucl. Chem.,* 2025, vol. 334, no. 3, pp. 2131–2138.